



Published in final edited form as:

*J Biomed Mater Res A*. 2011 March 1; 96(3): 520–527. doi:10.1002/jbm.a.33000.

## PLGA-chitosan/PLGA-alginate Nanoparticle Blends as Biodegradable Colloidal Gels for Seeding Human Umbilical Cord Mesenchymal Stem Cells

Qun Wang<sup>a</sup>, Syed Jamal<sup>b</sup>, Michael S. Detamore<sup>a</sup>, and Cory Berkland<sup>a,c,\*</sup>

<sup>a</sup> Department of Chemical and Petroleum Engineering, University of Kansas, Lawrence, KS 66047

<sup>b</sup> Department of Molecular Biosciences, University of Kansas, Lawrence, KS 66047

<sup>c</sup> Department of Pharmaceutical Science, University of Kansas, Lawrence, KS 66047

### Abstract

The natural polymers chitosan and alginate represent an attractive material choice for biodegradable implants. These were used as coating materials to make positively and negatively charged PLGA nanoparticles, respectively. After blending at total solids concentration >10% wt/vol, these oppositely charged nanoparticles yielded a cohesive colloidal gel. Electrostatic forces between oppositely charged nanoparticles produced a stable 3-D porous network that may be extruded or molded to the desired shape. This high concentration colloidal system demonstrated shear-thinning behavior due to the disruption of interparticle interactions. Once the external force was removed, the cohesive property of the colloidal gel was recovered. Scanning electron micrographs of dried colloidal networks revealed an organized, 3-D microporous structure. Rheological studies were employed to probe the differences in plasticity and shear sensitivity of colloidal gels. Viability tests of hUCMSCs seeded on the colloidal gels also demonstrated the negligible cytotoxicity of the materials. All the results indicated the potential application of the biodegradable colloidal gels as an injectable scaffold in tissue engineering and drug release.

### Keywords

PLGA; natural polymers; colloidal gel; tissue engineering

### 1. Introduction

Injectable scaffolds have received attention due to their potential for avoiding the invasive surgery typically required for tissue implantation.<sup>1</sup> From a clinical perspective, the use of injectable materials is an attractive alternative to surgery as it reduces the risk of infection, scar formation, patient discomfort and the cost of treatment.<sup>2</sup> Injectable scaffolds may be applied to fill tissue defects of irregular size and shape. Next generation injectable scaffolds should exhibit modest viscosity upon administration to ensure retention at the defect site, and may benefit from an increase in viscosity upon placement. Recently, many scaffolds that stiffen or solidify *in vivo* have been applied as injectable tissue scaffolds.<sup>3–4</sup> Usually, injectable scaffolds are polymerized or chemically crosslinked to stiffen the material. In this way, scaffolds may form via an *in situ* reaction induced by the presence of water, heat, light

\*Corresponding author; Tel: +1-785-864-1455; Fax: +1-785-864-1454; berkland@ku.edu.

or other stimuli. During the process of solidification, however, toxic chemical agents are sometimes employed, which may adversely affect the scaffolds, destabilize encapsulated biomolecules, or pose toxicity concerns. So, new materials that may stiffen through interactions such as electrostatic forces, van der Waals attraction and steric hindrance are desirable in the applications.

Naturally occurring polymers exhibit multiple desirable properties as scaffolds in tissue engineering.<sup>5</sup> Depending on the material and the source, certain natural polymers have been identified as biodegradable, non-antigenic, non-toxic and biofunctional.<sup>6–9</sup> The hydrophilic properties of many of these molecules and ample functional groups for further modification also make natural polymers excellent candidates for biomedical applications.<sup>10–11</sup> Chitosan and alginate are two major naturally occurring polysaccharides which have been widely used as drug delivery systems and tissue scaffolds.<sup>12–15</sup> Chitosan is a natural cationic polymer obtained by deacetylating chitin comprising copolymers of  $\beta$  (1  $\rightarrow$  4)-glucosamine and N-acetyl-D-glucosamine. When chitosan is dissolved in a dilute acid solution, the amino groups become protonated and introduce positive charge to the polymer.<sup>16</sup> Alginate is a natural anionic polymer derived from brown sea algae. Alginate has carboxyl groups which may introduce negative charge to the polymer at appropriate pH.<sup>17</sup> These two natural polyelectrolyte can facilitate the formation of oppositely charged biomedical materials.

Colloidal gels with three-dimensional (3-D) microperiodic structures comprised of biodegradable materials were manufactured to overcome some of these limitations.<sup>18–19</sup> These colloidal systems were composed of oppositely-charged nanoparticles at high concentration and stiffen through interparticle interactions such as electrostatic forces and van der Waals attraction.<sup>20</sup> Colloidal gels exhibiting pseudoplastic behavior resulting from interparticle interactions can facilitate the fabrication of shape-specific macroscale materials with 3-D architectures.<sup>21–22</sup> Recent research in materials science has aimed to leverage these phenomena to achieve unique bulk material properties for many different applications.<sup>23–28</sup> The application of moldable colloidal gels towards generating tissues has also been proposed.<sup>29–30</sup>

Here, natural polymers were integrated into biodegradable colloidal gels and examined for their potential as injectable tissue scaffolds. Poly (D, L-lactic-co-glycolic acid) (PLGA) is a biocompatible and biodegradable polymer, which has been approved in pharmaceutical products and used in tissue engineering scaffolds.<sup>31–34</sup> Chitosan and alginate were employed as surface modifiers to make oppositely-charged PLGA nanoparticles. Cohesive colloidal gels were created by simply mixing the oppositely-charged PLGA nanoparticles at different ratios. These materials exhibited desirable rheological properties for facile injection as tissue scaffolds. Colloidal gels were also highly compatible with human umbilical cord mesenchymal stem cells (hUCMSCs), which further supported possible translation of these materials.

## 2. Materials and methods

### 2.1. Materials

All materials were purchased from Fisher Scientific Inc. unless otherwise stated. PLGA (75:25) (7525 DLG 2.5E) was purchased from Lakeshore Biomaterials. Chitosan (448869, DD (degree of deacetylation) was 75–85%,  $M_n$  was 612 kDa ) was obtained from Sigma-Aldrich Co., Alginate sodium ( $M_v= 1.6 \times 10^5$ , viscosity was 39 MPas in 1.0% solution at 20 °C) was purchased from FMC BioPolymer.

## 2.2. Preparation of charged PLGA nanoparticles

Oppositely-charged PLGA nanoparticles were prepared by a solvent diffusion method. 100 mg of PLGA was dissolved in 10 mL acetone and then the solution was added into chitosan (dissolved in 0.2% wt/vol acetic acid solution) or alginate (dissolved in deionized water) surfactant solution with different concentration (0.1%, 0.2%, 0.5% and 1.0%) through a syringe pump at constant rate (20 mL/h, 40 mL/h and 60 mL/h) under stirring at 200 rpm overnight to evaporate acetone. Nanoparticles were collected by centrifugation (Beckman Co., Avanti 30) (14,000 rpm, 15 min). The nanoparticles were resuspended using deionized water and centrifuged three times to remove excess chitosan or alginate. A fine powder of charged nanoparticles was obtained by lyophilization for ~2 days.

## 2.3. Preparation of colloidal gels

Lyophilized nanoparticles (PLGA-Chitosan or PLGA-Alginate) were dispersed in deionized water at the reported concentrations. These dispersions were mixed in different proportions to obtain the different weight ratios studied. Homogeneous colloid mixtures were prepared in a bath sonicator for 3 minutes and stored at 4 °C for 2 h to allow particles to be structurally organized before use. Several colloidal gels, with different mass ratios of PLGA-chitosan nanoparticles to PLGA-alginate nanoparticles, were designated as C100, CA37, CA55, CA73 and A100 (C: PLGA-chitosan nanoparticles; A: PLGA-alginate nanoparticles; the weight ratios of PLGA-chitosan nanoparticles to PLGA-alginate nanoparticles were 100:0, 30:70, 50:50, 70:30 and 0:100, respectively).

## 2.4. Characterization of nanoparticles and colloidal gels

The sizes and zeta potentials of the different PLGA nanoparticles were determined using a ZetaPALS dynamic light scattering system (Brookhaven, ZetaPALS). All samples were analyzed in triplicate. Scanning electron microscopy (SEM) was performed using a Jeol JSM-6380 field emission scanning electron microscope at an accelerating voltage of 10kV.

## 2.5. Rheological experiments

Rheological experiments were performed using a controlled stress rheometer (AR2000, TA Instrument Ltd.). 2° cone steel plates (20 mm diameter) were used and the 500 μm gap was filled with tested colloidal gel. A solvent trap was used to prevent evaporation of water. The viscoelastic properties of the sample were determined at 20 °C by forward-and-backward stress sweep experiments. The viscosity ( $\eta$ ) was monitored while the stress was increased and then decreased (frequency = 1 Hz) in triplicate with 10 minutes between cycles. The gel recoverability was assessed using defined time breaks between cycles. All samples were analyzed in triplicate.

## 2.6. Cytotoxicity

hUCMSCs were harvested and cultured until passage 2 as previously described<sup>35</sup> for cell seeding in culture medium, which included low glucose Dulbecco's Modified Eagle's Medium, 10% FBS, and penicillin/streptomycin (PS). Then, hUCMSCs were seeded at a density of  $1 \times 10^4$  cells per  $\text{cm}^2$ . Cells were grown to near confluence in the individual wells of a 12-well tissue culture-treated plate and then exposed to 100, 200, and 300 μl of colloidal gel. The working concentrations of the nanoparticles used were as follows: PLGA 2 mg/ml; chitosan 30 mg/ml; and alginate 30 mg/ml. Cells were cultured on the colloidal gels for 48 hours and 2 weeks, the media being carefully changed every 2–3 days without disturbing the settled gels at the bottom. Subsequently, the cells were stained with LIVE/DEAD reagent (dye concentration 2 mM calcein AM, 4 mM ethidium homodimer-1; Molecular Probes) and incubated for 45 mins, before being subjected to fluorescence microscopy (Nikon TS 100 with Epifluorescence Attachment).

### 3. Results and discussion

#### 3.1. PLGA nanoparticles were coated with natural biopolymers

The entire process for the fabrication of PLGA nanoparticle colloidal gels is illustrated in Figure 1. In the first step, PLGA nanoparticles were prepared by a solvent diffusion method. The precipitation of PLGA nanoparticles occurred in the respective polyelectrolyte solution, chitosan or alginate, resulting in a coating of either polymer on the nanoparticle surface. Chitosan introduced positive charge and alginate introduced negative charge on the surface of PLGA nanoparticles. The particle sizes (Figure 2) and zeta potentials (Figure 3) of each particle type depended on the synthesis conditions. The injection rate of the dissolved PLGA and the concentration of the biopolymer solution were two key factors influencing the sizes and zeta potentials of the nanoparticles.

During the fabrication process, PLGA precipitated to form nanoparticles as the organic solvent mixed with water. The faster injection rate resulted in a higher local concentration of PLGA at the needle tip, therefore, larger nanoparticles were produced (Figure 2). In addition, the concentration of biopolymer solution (chitosan or alginate) determined the magnitude of the nanoparticle surface charge. Increasing the concentration of biopolymer solution induced a higher charge on the nanoparticles, since presumably more polyelectrolyte was associated with the nanoparticle surface (Figure 3). In order to balance the particle sizes and zeta potentials of the two oppositely charged particles, 248.5±11.9 nm PLGA-chitosan nanoparticles with a zeta potential of +18.8±3.2 mV and 181.6±3.3 nm PLGA-alginate nanoparticles with a zeta potential of -23.4±1.2 mV were prepared for colloidal gel experiments by injecting PLGA solution into 0.2% polyelectrolyte solution at a constant rate of 40 mL/h. The optimized nanoparticles were collected and used to prepare colloidal gels.

#### 3.2. PLGA colloidal gels exhibited microporous structures and shape retention

For initial studies, cationic or anionic nanoparticles were suspended in deionized water at 20% (w/w) at room temperature. SEM pictures of dried colloidal networks revealed little difference in the structure of dried gels containing different mass ratios of oppositely-charged nanoparticles (Figure 4). After drying, all mass ratios (3:7, 1:1, and 7:3; PLGA-chitosan: PLGA-alginate) exhibited a loosely organized, microporous structure. The oppositely-charged nanoparticles were linked together to form micrometer-scale, ring-like structures with microchannels, which interconnected to form the bulk porous structure observed. Domains of more tightly packed nanoparticle agglomerates were evident, suggesting that the cohesive nature of colloidal gels results from the equilibrium of interparticle attractions (tight agglomerates) and repulsions (pores).

Colloidal gels composed of oppositely-charged nanoparticles at high concentration exhibit unique pseudoplastic properties facilitating the fabrication of shape-specific microscale materials. In this project, the pseudoplastic behavior of colloidal gels was leveraged to construct tissue engineering scaffolds of the desired shape (Figure 5). The colloidal gels kept their shape for several hours unless changed by an external force. The colloidal gels with different compositions showed slight differences in moldability due to the different ratios of oppositely charged PLGA nanoparticles. Colloidal gel composed of a more equal overall charge balance (CA55 with 1:1 mass ratio, Figure 5B) exhibited less fluidity and better shape stability. Pure nanoparticles at the same concentration showed no moldability (pure PLGA-chitosan nanoparticles, Figure 5D). Results confirmed that the overall charge ratio determined the bulk and microscopic structures and properties of the colloidal system.<sup>36</sup> In this research, the small size and high charge of the PLGA nanoparticles were leveraged to form stable colloidal gels.

### 3.3. PLGA colloidal gels were shear thinning with recoverable stiffness

Rheological studies were employed to probe the differences in viscoelasticity of colloidal gels. Equal mass ratios of nanoparticles yielded the highest viscosity gel and improved reversibility compared to other ratios (Figure 6). As expected, colloidal gels containing more positively-charged particles (CA73, 7:3 mass ratio, 20% concentration) exhibited higher viscosity, while colloidal gels composed of excess negatively-charged particles (CA37, 3:7 mass ratio, 20% concentration) exhibited more fluidity. The larger zeta potential of negatively charged nanoparticles resulted in a more equal overall charge balance when positively charged particles were in excess, thus, providing a probable explanation for the stronger cohesion and enhanced reversibility observed in the 7:3 mass ratio compared to the 3:7 mass ratio. Pure nanoparticle suspensions exhibited minimal shear-thinning behavior (C100 and A100).

The viscosity of colloidal gel was enhanced and shear-thinning more pronounced as the concentration of nanoparticles increased (Figure 7). Consecutive acceleration/deceleration cycles of the shear force applied to CA55 colloidal gels (20% concentration) revealed that these materials did not rapidly recover (Figure 8). Delaying shear cycles for more time may enhance the recovery of gel viscosity. All the results suggested that the colloidal gels were desirable for injectable applications.

For colloidal gels, the strength of the cohesion depends upon the interparticle interactions such as electrostatic forces and van der Waals attractions.<sup>20</sup> These interparticle interactions were controlled by the composition of the colloidal gels, such as concentration and ratio of the two oppositely-charged particles. PLGA-chitosan and PLGA-alginate nanoparticles self-assembled through interparticle interactions resulting in a stable 3-D porous network. Under static conditions, the viscosity and structure of colloidal assemblies leading to a stable structure exhibiting high viscosity at equilibrium (Figure 5, A–C). If the particle-particle equilibrium is disrupted, e.g. by external force applied to disrupt the interparticle interactions, the colloidal system will demonstrate shear-thinning behavior. Once the external force is removed, the strong cohesive property of the colloidal gel is recovered and the 3D porous structure is reconstructed. This reversibility makes the gel an excellent material for applications in molding, extrusion, or injection of tissue scaffolds and drug delivery systems.

### 3.4. PLGA colloidal gels had negligible cytotoxicity to hUCMSCs

Stem cell based tissue engineering has the potential to revolutionize biomedicine with the ability to repair or regenerate the damaged or diseased tissue.<sup>37–38</sup> hUCMSCs are multipotent, able to differentiate into adipocytes, osteoblasts, chondrocytes, neurons, and other cells.<sup>39–42</sup> Comparing to other stem cells, hUCMSCs are advantageous because umbilical cords can be collected at a low cost and represent an inexhaustible stem cell source. hUCMSCs can be harvested from discarded umbilical cords, expanded in culture, induced to differentiate and combined with a scaffold to repair tissue defects.<sup>43–44</sup> However, pre-formed carriers for cell delivery have drawbacks including the difficulties in seeding the cells on the scaffold, biocompatibility between the cells and the scaffolds, and placement in minimally invasive surgeries.<sup>45</sup> In this research, biodegradable PLGA colloidal gels were used to overcome these difficulties.

hUCMSCs were harvested and cultured on CA55 and CA37 colloidal gels for up to two weeks, following which, viability assays were conducted. The Live/Dead Cytotoxicity Assay Kit from Molecular Probes was employed, which uses two probes, namely Calcein AM and Ethidium Bromide homodimer, to identify two critical matrices of cell viability: (a) protease activity and (b) membrane integrity. The membrane-permeable dye Calcein/AM

(Ex495nm/Em515nm) was hydrolyzed by cellular proteases, ubiquitous in living cells, to yield a green fluorescent product; on the contrary, ethidium homodimer (Ex495/Em635nm) only entered the cell membranes of dead or dying cells to bind the DNA, undergoing a manifold enhancement in red fluorescence (Figure 9). Very little cell death was observed in cells treated with PLGA nanoparticles for 48 hours and for 2 weeks. On the other hand, when 70 % ethanol was used as a negative control, appreciably higher numbers of dead cells were observed. The live/dead experiments qualitatively demonstrated that PLGA colloidal gels possessed little cytotoxicity towards hUCMSCs, which suggested that the material may be used as a scaffold for seeding stem cells.

#### 4. Conclusions

In this paper, a new colloidal gel made by oppositely-charged PLGA nanoparticles coated with naturally occurring polyelectrolytes was reported. The cohesive strength of the colloidal gels resulted from the interparticle interactions between the oppositely-charged nanoparticles. The shear sensitivity to external force and recoverable pseudoplastic property make it an excellent injectable biomaterial. Cytotoxicity tests of the colloidal gels also demonstrated negligible toxicity to hUCMSCs. Thus, injectable PLGA colloidal gels represent a promising new material for tissue engineering. In further research, integration of controlled release of active ingredients (*e.g.* growth factors) will allow for advanced combination strategies for tissue engineering coupled with drug release.

#### Acknowledgments

We gratefully acknowledge Prof. Stevin Gehrke for the use of equipment and the Microscopy Laboratory for assistance with imaging. We are grateful for support from funding agencies such as the NIH (1R03 AR054035-01A1, P20 RR016443 and P20 RR015563 (CB)) and State of Kansas. We also extend our indebtedness to the nursing staff at Lawrence Memorial Hospital, Lawrence, Kansas, for their kind assistance with umbilical cord harvesting.

#### References

1. Lee J, Cuddihy M, Kotov N. Three-dimensional cell culture matrices: state of the art. *Tissue Engineering Part B: Reviews*. 2008; 14(1):61–86. [PubMed: 18454635]
2. Hou Q, Bank P, Shakesheff K. Injectable scaffolds for tissue regeneration. *Journal of Materials Chemistry*. 2004; 14(13):1915–1923.
3. Cushing M, Anseth K. MATERIALS SCIENCE: Hydrogel cell cultures. *Science*. 2007; 316(5828): 1133–1134. [PubMed: 17525324]
4. Wang Q, Wang J, Lu Q, Detamore M, Berklund C. Injectable PLGA based colloidal gels for zero-order dexamethasone release in cranial defects. *Biomaterials*. 2010; 31(18):4980–4986. [PubMed: 20303585]
5. Malafaya P, Silva G, Reis R. Natural-origin polymers as carriers and scaffolds for biomolecules and cell delivery in tissue engineering applications. *Advanced drug delivery reviews*. 2007; 59(4–5): 207–233. [PubMed: 17482309]
6. Li Z, Ramay H, Hauch K, Xiao D, Zhang M. Chitosan-alginate hybrid scaffolds for bone tissue engineering. *Biomaterials*. 2005; 26(18):3919–3928. [PubMed: 15626439]
7. Williams S, Wang Q, MacGregor R, Siahaan T, Stehno-Bittel L, Berklund C. Adhesion of pancreatic beta cells to biopolymer films. *Biopolymers*. 2009; 91(8):676–685. [PubMed: 19353639]
8. Wang Q, Du Y, Fan L. Properties of chitosan/poly (vinyl alcohol) films for drug-controlled release. *Journal of Applied Polymer Science*. 2005; 96(3):808–813.
9. Wang Q, Du Y, Hu X, Yang J, Fan L, Feng T. Preparation of alginate/soy protein isolate blend fibers through a novel coagulating bath. *Journal of Applied Polymer Science*. 2006; 101(1):425–431.

10. Chen G, Ushida T, Tateishi T. A biodegradable hybrid sponge nested with collagen microsponges. *Journal of Biomedical Materials Research Part A*. 2000; 51(2):273–279.
11. Lahiji A, Sohrabi A, Hungerford D, Frondoza C. Chitosan supports the expression of extracellular matrix proteins in human osteoblasts and chondrocytes. *Journal of Biomedical Materials Research Part A*. 2000; 51(4):586–595.
12. Wang Q, Zhang N, Hu X, Yang J, Du Y. Chitosan/starch fibers and their properties for drug controlled release. *European journal of pharmaceutics and biopharmaceutics*. 2007; 66(3):398–404. [PubMed: 17196808]
13. Francis Suh J, Matthew H. Application of chitosan-based polysaccharide biomaterials in cartilage tissue engineering: a review. *Biomaterials*. 2000; 21(24):2589–2598. [PubMed: 11071608]
14. Wang Q, Zhang N, Hu X, Yang J, Du Y. Alginate/polyethylene glycol blend fibers and their properties for drug controlled release. *Journal of Biomedical Materials Research Part A*. 2007; 82(1):122–128. [PubMed: 17269140]
15. Becker T, Kipke D, Brandon T. Calcium alginate gel: a biocompatible and mechanically stable polymer for endovascular embolization. *Journal of Biomedical Materials Research Part A*. 2001; 54(1):76–86.
16. Mao H, Roy K, Troung-Le V, Janes K, Lin K, Wang Y, August J, Leong K. Chitosan-DNA nanoparticles as gene carriers: synthesis, characterization and transfection efficiency. *Journal of controlled release*. 2001; 70(3):399–421. [PubMed: 11182210]
17. Aslani P, Kennedy R. Studies on diffusion in alginate gels. I. Effect of cross-linking with calcium or zinc ions on diffusion of acetaminophen. *Journal of controlled release*. 1996; 42(1):75–82.
18. Griffith L, Naughton G. Tissue engineering--current challenges and expanding opportunities. *Science*. 2002; 295(5557):1009. [PubMed: 11834815]
19. Li Y, Cunin F, Link J, Gao T, Betts R, Reiver S, Chin V, Bhatia S, Sailor M. Polymer replicas of photonic porous silicon for sensing and drug delivery applications. *Science*. 2003; 299(5615):2045. [PubMed: 12663921]
20. Tohver V, Chan A, Sakurada O, Lewis J. Nanoparticle engineering of complex fluid behavior. *Langmuir*. 2001; 17(26):8414–8421.
21. Johnson S, Ollivier P, Mallouk T. Ordered mesoporous polymers of tunable pore size from colloidal silica templates. *Science*. 1999; 283(5404):963. [PubMed: 9974384]
22. Holtz J, Asher S. Polymerized colloidal crystal hydrogel films as intelligent chemical sensing materials. *Nature*. 1997; 389(6653):829–832. [PubMed: 9349814]
23. Theriault D, White S, Lewis J. Chaotic mixing in three-dimensional microvascular networks fabricated by direct-write assembly. *Nature Materials*. 2003; 2(4):265–271.
24. Chrisey D. *MATERIALS PROCESSING: The Power of Direct Writing*. Science (New York, NY). 2000; 289(5481):879.
25. Klajn R, Bishop K, Fialkowski M, Paszewski M, Campbell C, Gray T, Grzybowski B. Plastic and moldable metals by self-assembly of sticky nanoparticle aggregates. *Science*. 2007; 316(5822):261–264. [PubMed: 17431176]
26. Niemeyer C. Functional hybrid devices of proteins and inorganic nanoparticles. *Angewandte Chemie International Edition*. 2003; 42(47):5796–5800.
27. Hu Z, Lu X, Gao J. Hydrogel opals. *Advanced Materials*. 2001; 13(22):1708–1712.
28. Katz E, Willner I. Integrated nanoparticle-biomolecule hybrid systems: synthesis, properties, and applications. *Angewandte Chemie International Edition*. 2004; 43(45):6042–6108.
29. Xie B, Parkhill R, Warren W, Smay J. Direct writing of three-dimensional polymer scaffolds using colloidal gels. *Advanced Functional Materials*. 2006; 16(13):1685–1693.
30. Dellinger J, Cesarano J III, Jamison R. Robotic deposition of model hydroxyapatite scaffolds with multiple architectures and multiscale porosity for bone tissue engineering. *Journal of Biomedical Materials Research Part A*. 2007; 82(2):383–394. [PubMed: 17295231]
31. Wang Q, Wang L, Detamore M, Berkland C. Biodegradable colloidal gels as moldable tissue engineering scaffolds. *Advanced Materials*. 2008; 20(2):236–239.

32. Kim D, Martin D. Sustained release of dexamethasone from hydrophilic matrices using PLGA nanoparticles for neural drug delivery. *Biomaterials*. 2006; 27(15):3031–3037. [PubMed: 16443270]
33. Brigger I, Dubernet C, Couvreur P. Nanoparticles in cancer therapy and diagnosis. *Advanced drug delivery reviews*. 2002; 54(5):631–651. [PubMed: 12204596]
34. Anderson J, Shive M. Biodegradation and biocompatibility of PLA and PLGA microspheres. *Advanced drug delivery reviews*. 1997; 28(1):5–24. [PubMed: 10837562]
35. Weiss M, Medicetty S, Bledsoe A, Rachakatla R, Choi M, Merchav S, Luo Y, Rao M, Velagaleti G, Troyer D. Human umbilical cord matrix stem cells: preliminary characterization and effect of transplantation in a rodent model of Parkinson's disease. *Stem Cells*. 2006; 24(3):781–792. [PubMed: 16223852]
36. Gilchrist J, Chan A, Weeks E, Lewis J. Phase Behavior and 3D Structure of Strongly Attractive Microsphere- Nanoparticle Mixtures. *Langmuir*. 2005; 21(24):11040–11047. [PubMed: 16285769]
37. Datta N. In vitro generated extracellular matrix and fluid shear stress synergistically enhance 3D osteoblastic differentiation. *Proceedings of the National Academy of Sciences of the United States of America*. 2006; 103(8):2488–2493. [PubMed: 16477044]
38. Yao J, Radin S, Reilly G, Leboy P, Ducheyne P. Solution-mediated effect of bioactive glass in poly (lactic-co-glycolic acid)-bioactive glass composites on osteogenesis of marrow stromal cells. *Journal of Biomedical Materials Research Part A*. 2005; 75(4):794–801. [PubMed: 16138322]
39. Wang H, Hung S, Peng S, Huang C, Wei H, Guo Y, Fu Y, Lai M, Chen C. Mesenchymal stem cells in the Wharton's jelly of the human umbilical cord. *Stem Cells*. 2004; 22(7):1330–1337. [PubMed: 15579650]
40. Can A, Karahuseyinoglu S. Concise review: human umbilical cord stroma with regard to the source of fetus-derived stem cells. *Stem Cells*. 2007; 25(11):2886–2895. [PubMed: 17690177]
41. Baksh D, Yao R, Tuan R. Comparison of proliferative and multilineage differentiation potential of human mesenchymal stem cells derived from umbilical cord and bone marrow. *Stem Cells*. 2007; 25(6):1384–1392. [PubMed: 17332507]
42. Karahuseyinoglu S, Kocafe C, Balci D, Erdemli E, Can A. Functional structure of adipocytes differentiated from human umbilical cord stroma-derived stem cells. *Stem Cells*. 2008; 26(3):682–691. [PubMed: 18192234]
43. Bailey M, Wang L, Bode C, Mitchell K, Detamore M. A comparison of human umbilical cord matrix stem cells and temporomandibular joint condylar chondrocytes for tissue engineering temporomandibular joint condylar cartilage. *Tissue engineering*. 2007; 13(8):2003–2010. [PubMed: 17518722]
44. Kretlow J, Young S, Klouda L, Wong M, Mikos A. Injectable biomaterials for regenerating complex craniofacial tissues. *Advanced Materials*. 2009; 21(32–33):3368–3393. [PubMed: 19750143]
45. Laurencin C, Ambrosio A, Borden M, Cooper J Jr. Tissue engineering: orthopedic applications. *Annual review of biomedical engineering*. 1999; 1(1):19–46.

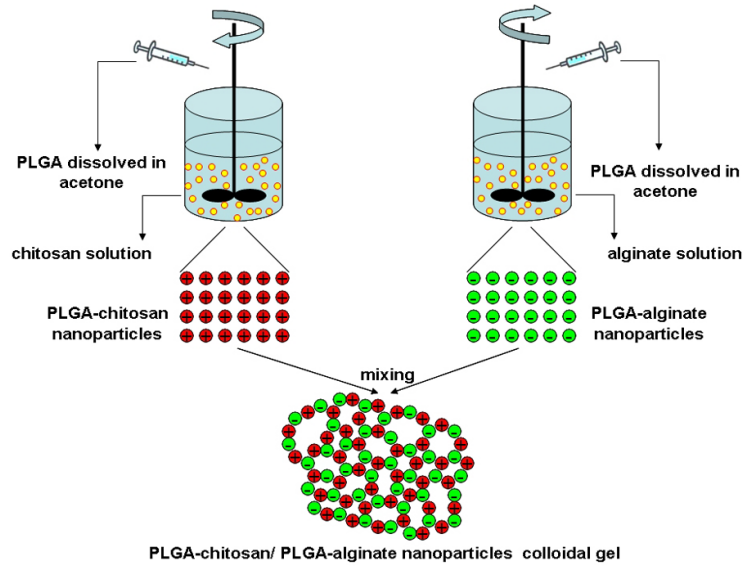


**Figure 1.** Schematic presentation of the process for fabrication of oppositely charged PLGA nanoparticles and formation of colloidal gel.

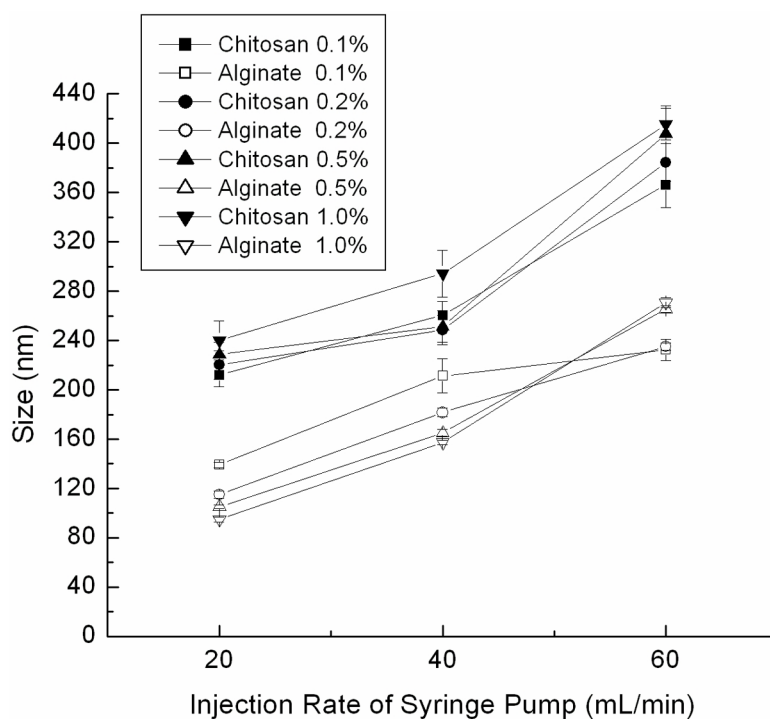


**Figure 2.** Sizes of PLGA nanoparticles made in chitosan or alginate solution with different concentrations (0.1%, 0.2%, 0.5% and 1.0%) at different injection rates (20 mL/h, 40 mL/h and 60 mL/h) by syringe pump.

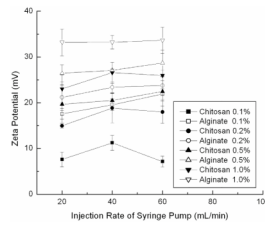


**Figure 3.**

Zeta potentials of PLGA nanoparticles made in chitosan or alginate solution with different concentration (0.1%, 0.2%, 0.5% and 1.0%) at different injection rates ( 20 mL/h, 40 mL/h and 60 mL/h) by syringe pump (chitosan embued positive charge and alginate embued negative charge).

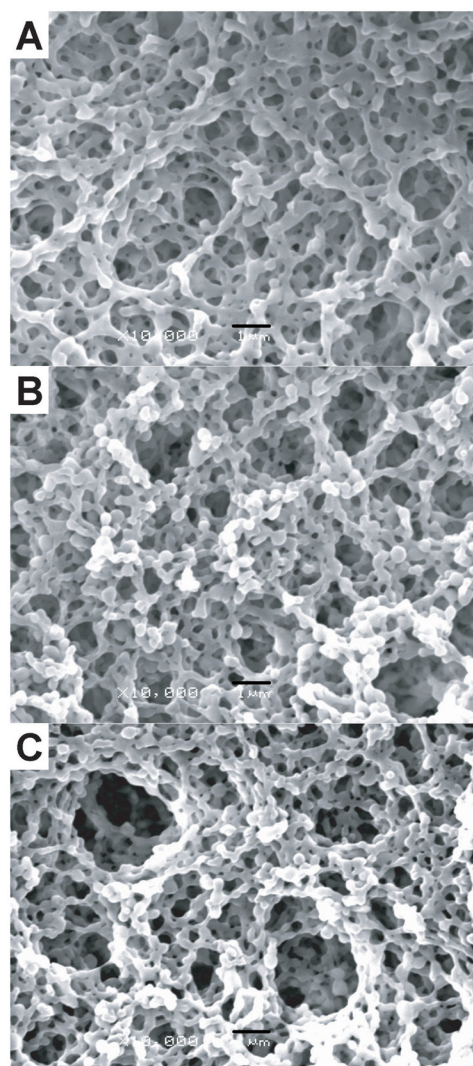


**Figure 4.** SEM images of colloidal gels (A) CA37, (B) CA55 and (C) CA73 (scale bar = 1 $\mu$ m).

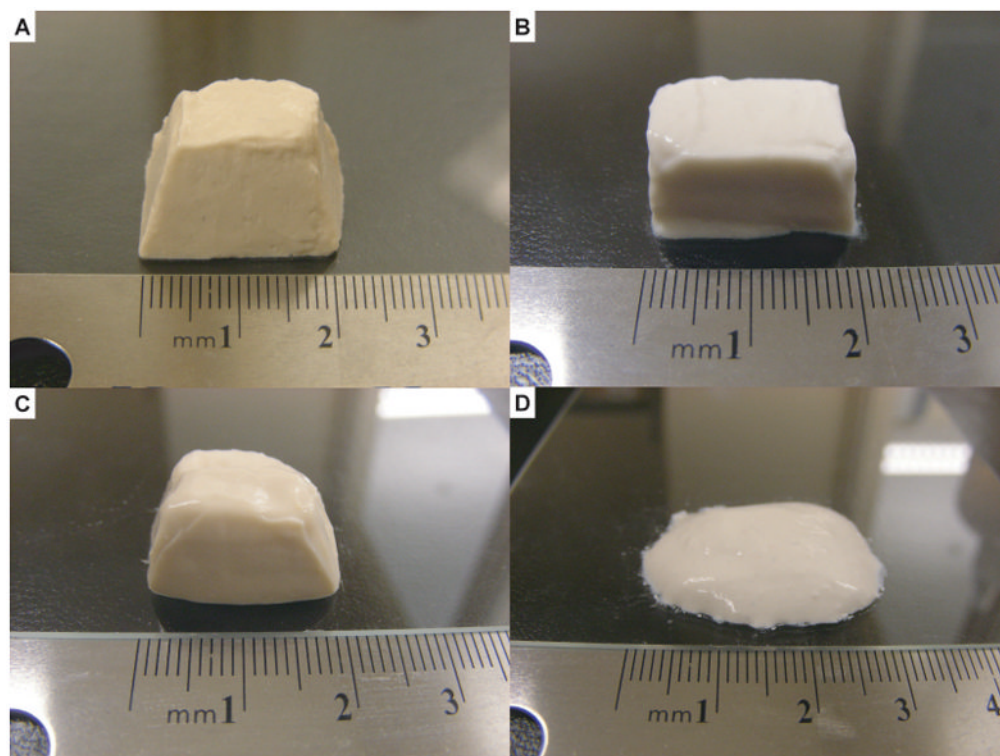


**Figure 5.** Shaped tissue scaffolds made by colloidal gels (A) CA37, (B) CA55, (C) CA73 and (D) pure PLGA-chitosan nanoparticles.

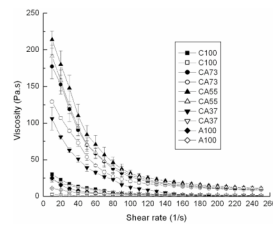


**Figure 6.** Viscosity and shear-thinning behavior of colloidal gels (20% concentration) mixed at different ratios for accelerating (solid symbols) and decelerating (open symbols) shear force.

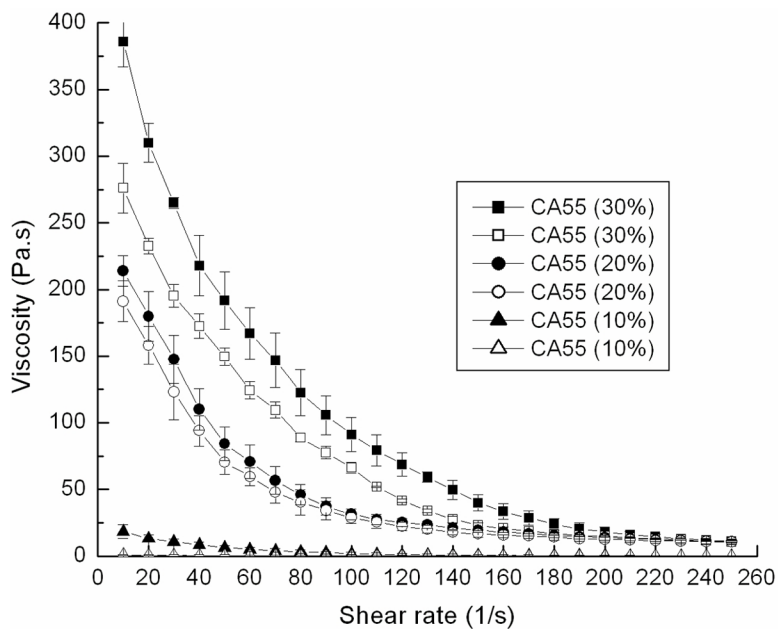


**Figure 7.** Viscosity and shear-thinning behavior of CA55 colloidal gel at different concentrations for accelerating (solid symbols) and decelerating (open symbols) shear force when no recovery time was allowed between shear cycles.

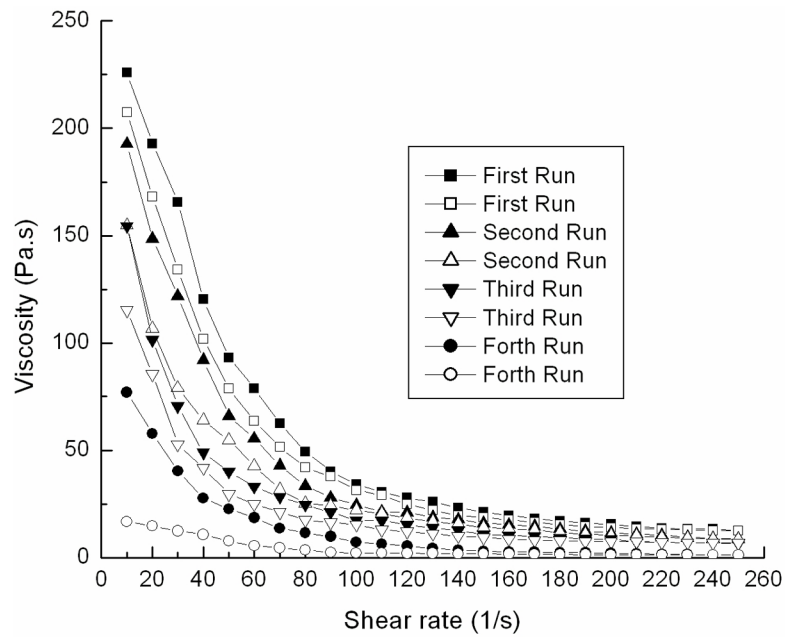


**Figure 8.** Viscosity and shear-thinning behavior of CA55 colloidal gel (20% concentration) for repeated accelerating (solid symbols) and decelerating (open symbols) shear force when no recovery time was allowed between shear cycles.

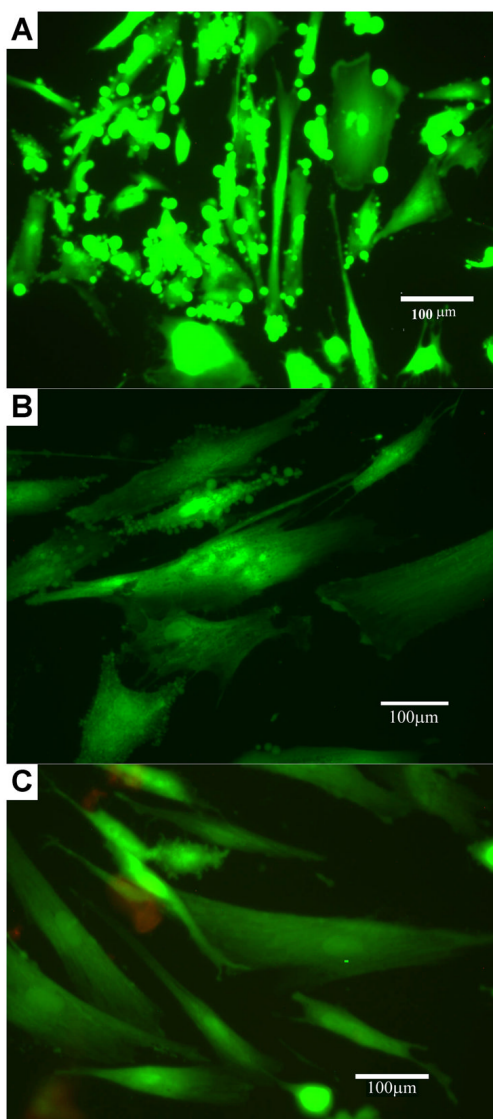


**Figure 9.** Human umbilical cord matrix stem cells cultured on colloidal gels CA 55 (B) and CA37 (C) demonstrated high viability (green) and minimal cell death (red) comparing to reference (A, treated without colloidal gels).